

See discussions, stats, and author profiles for this publication at: <https://www.researchgate.net/publication/259722735>

# Divalent Heteroleptic Ytterbium Complexes – Effective Catalysts for Intermolecular Styrene Hydrophosphination and Hydroamination

ARTICLE in INORGANIC CHEMISTRY · JANUARY 2014

Impact Factor: 4.76 · DOI: 10.1021/ic4027859 · Source: PubMed

CITATIONS

13

READS

25

8 AUTHORS, INCLUDING:



**Sorin-Claudiu Roșca**

Université de Rennes 1

5 PUBLICATIONS 52 CITATIONS

SEE PROFILE



**Yann Sarazin**

Université de Rennes 1

62 PUBLICATIONS 1,472 CITATIONS

SEE PROFILE



**Jean-François Carpentier**

Université de Rennes 1

309 PUBLICATIONS 7,681 CITATIONS

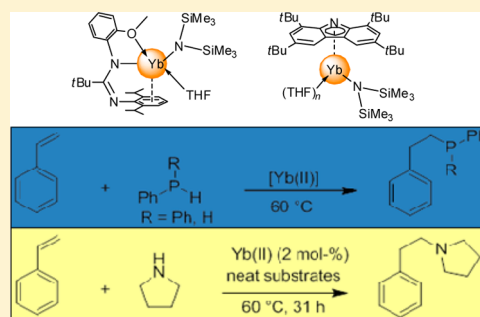
SEE PROFILE

## Divalent Heteroleptic Ytterbium Complexes – Effective Catalysts for Intermolecular Styrene Hydrophosphination and Hydroamination

Ivan V. Basalov,<sup>†</sup> Sorin Claudiu Roșca,<sup>‡</sup> Dmitry M. Lyubov,<sup>†</sup> Alexander N. Selikhov,<sup>†</sup> Georgy K. Fukin,<sup>†</sup> Yann Sarazin,<sup>‡</sup> Jean-François Carpentier,<sup>\*,‡</sup> and Alexander A. Trifonov<sup>\*,†</sup><sup>†</sup>G. A. Razuvaev Institute of Organometallic Chemistry of Russian Academy of Sciences, Nizhny Novgorod, Russia<sup>‡</sup>Organometallics: Materials and Catalysis, Institut des Sciences Chimiques de Rennes, UMR 6226 CNRS – Université de Rennes 1, Rennes, France

## Supporting Information

**ABSTRACT:** New heteroleptic Yb(II)–amide species supported by amidinate and 1,3,6,8-tetra-*tert*-butylcarbazol-9-yl ligands [2-MeOC<sub>6</sub>H<sub>4</sub>NC(*t*Bu)N-(C<sub>6</sub>H<sub>3</sub>-*i*Pr<sub>2</sub>-2,6)]YbN(SiMe<sub>3</sub>)<sub>2</sub>(THF) (**6**) and [1,3,6,8-*t*Bu<sub>4</sub>C<sub>12</sub>H<sub>4</sub>N]Yb[N-(SiMe<sub>3</sub>)<sub>2</sub>](THF)<sub>*n*</sub> (*n* = 1 (**7**), 2 (**8**)) were synthesized using the amine elimination approach. Complex **6** features an unusual  $\kappa^1\text{-N}, \kappa^2\text{-O}, \eta^6\text{-arene}$  coordination mode of the amidinate ligand onto Yb(II). Complexes **7** and **8** represent the first examples of lanthanide complexes with  $\pi$ -coordination of carbazol-9-yl ligands. Complexes **6** and **7**, as well as the amidinate–Yb(II)–amide [tBuC(NC<sub>6</sub>H<sub>3</sub>-*i*Pr<sub>2</sub>-2,6)<sub>2</sub>]YbN(SiMe<sub>3</sub>)<sub>2</sub>(THF) (**5**), are efficient precatalysts for the intermolecular hydrophosphination and hydroamination of styrene with diphenylphosphine, phenylphosphine, and pyrrolidine to give exclusively the anti-Markovnikov monoaddition product. For both types of reaction, the best performances were observed with carbazol-9-yl complex **7** (TONs up to 92 and 48 mol/mol at 60 °C, respectively).



## INTRODUCTION

Extensive research activity pursued over the past three decades in the field of organic derivatives of trivalent lanthanides has revealed their high potential as catalysts (or precatalysts) for various transformations involving unsaturated substrates, e.g., polymerization,<sup>1</sup> hydrogenation,<sup>2</sup> hydrosilylation,<sup>3</sup> hydroamination,<sup>4</sup> hydrophosphination,<sup>5</sup> hydroalkoxylation,<sup>6</sup> hydrothiolation,<sup>6</sup> and hydroboration.<sup>7</sup> Besides, the catalytic properties of divalent lanthanide complexes still remain poorly explored<sup>8</sup> despite larger ionic radii<sup>9</sup> and pronounced reductive properties,<sup>10</sup> which make them promising candidates for catalytic applications. Among these, hydroelementation reactions, that is, the addition of E–H (E = N, P...) functionalities across C–C multiple bonds, are atom-economic processes for the synthesis of valuable compounds that may be one of the prospective application fields of such divalent lanthanide complexes. Much progress has been done in the area of lanthanide-promoted intramolecular hydroamination and hydrophosphination; however, success is somewhat elusive for the intermolecular version of these transformations.<sup>11</sup> Recent achievements in intermolecular hydroelementation reactions promoted by calcium complexes,<sup>12</sup> whose ionic radius is similar to that of Yb(II),<sup>9</sup> prompted us to evaluate the catalytic activity of heteroleptic Yb(II)–amides in intermolecular olefin hydrophosphination and hydroamination. Herein, we report on the synthesis, characterization, and catalytic activity of a series of heteroleptic Yb(II)–amides supported by various multidentate N-based

ligands in intermolecular hydrophosphination and hydroamination of styrene.

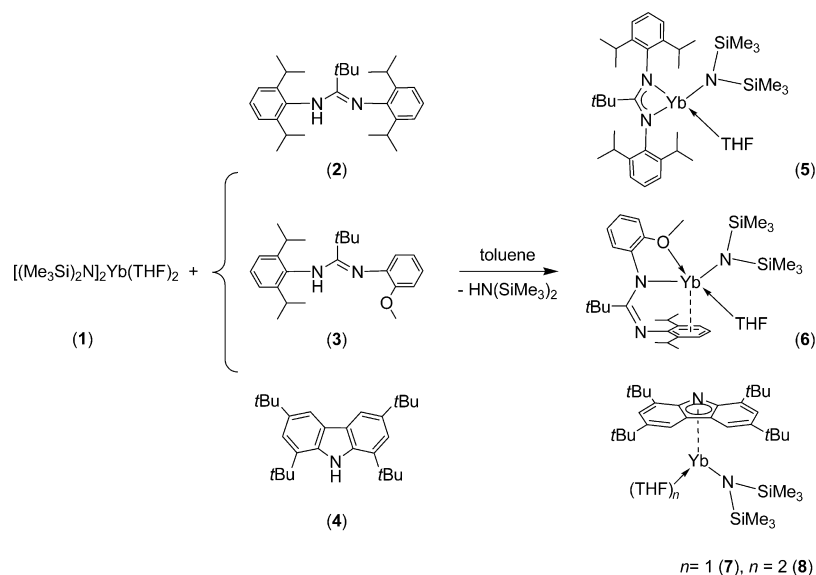
## RESULTS AND DISCUSSION

**Synthesis and Characterization of Divalent Ytterbium Complexes.** Amine elimination from Yb(II)–bis-(trimethylsilylamide), [(Me<sub>3</sub>Si)<sub>2</sub>N]<sub>2</sub>Yb(THF)<sub>2</sub> (**1**)<sup>13</sup>—a readily available precursor that can be prepared on a multigram scale—was used for the synthesis of a series of heteroleptic Yb(II)–amide complexes supported by N-containing ligands (Scheme 1). The reactions of equimolar amounts of **1** and proligands **2**–**4** were carried out in toluene at ambient temperature or under moderate heating (70 °C). The synthesis and characterization of [tBuC(NC<sub>6</sub>H<sub>3</sub>-*i*Pr<sub>2</sub>-2,6)<sub>2</sub>]Yb[N-(SiMe<sub>3</sub>)<sub>2</sub>](THF) (**5**) have been published recently.<sup>14</sup> All reactions occur with a release of one equivalent of HN(SiMe<sub>3</sub>)<sub>2</sub>, which was eventually detected and quantified by <sup>1</sup>H NMR spectroscopy and GLC. Evaporation of volatiles under a vacuum and subsequent recrystallization of the residual solids from hexane afforded the new complexes **6** and **7** in 78% and 90% yields, respectively. Slow cooling of a solution of the reaction product of **1** and **4** in a toluene–THF (20:1) mixture at –30 °C allowed for the isolation of bis-THF adduct **8** in 63% yield.

Received: November 6, 2013

Published: January 14, 2014

Scheme 1



Complexes 6–8 are highly air- and moisture-sensitive crystals, well soluble in aliphatic and aromatic hydrocarbons. As evidenced by NMR spectroscopy, complexes 6–8 are diamagnetic, in line with the divalent oxidation state of the ytterbium atom.

Complex 6 crystallizes with two crystallographically independent molecules in the asymmetric unit as established by an X-ray diffraction study. The solid-state structure of 6 reveals that introduction of an additional Lewis base group (i.e., OMe) into one of the aryl substituents of the NCN core leads to a dramatic change in the coordination mode of the amidinate ligand (Figure 1). In fact, in complex 5, the bidentate amidinate ligand adopts a classic  $\kappa^2\text{-N,N'}$ -chelating coordination mode,<sup>14</sup> while in 6 the monoanionic tridentate amidinate ligand coordinates to Yb(II) in an unusual  $\kappa^1\text{-N}, \kappa^2\text{-O}, \eta^6\text{-arene}$  fashion.  $\kappa^1\text{-N}, \eta^6\text{-arene}$  coordination to ytterbium has been previously documented for Yb(II) complexes with bulky guanidinate and amidinate ligands<sup>14,15</sup> while, to our knowledge,  $\kappa^1\text{-N}, \kappa^2\text{-O}, \eta^6\text{-arene}$  coordination fashion is described here for the first time. Besides the tridentate amidinate ligand, the Yb(II) center in 6 is bound to one monoanionic  $\text{N}(\text{SiMe}_3)_2^-$  group and the oxygen atom of the THF molecule. The formal coordination number of Yb(II) in 6 is thus seven. The Yb– $\text{N}_{\text{amidinate}}$  and Yb– $\text{Ar}_{\text{centroid}}$  distances in 6 (2.452(2) and 2.695(3) Å) are expectedly longer compared to those in the related six-coordinate Yb(II) complexes with  $\kappa^1\text{-N}, \eta^6\text{-arene}$  coordination [ $\{t\text{BuC}(\text{NC}_6\text{H}_3\text{-}2,6\text{-iPr}_2)_2\}\text{Yb}(\mu\text{-H})_2$ ] (2.329(3), 2.420(4) Å),<sup>14</sup> [ $\{t\text{BuC}(\text{NC}_6\text{H}_3\text{-}2,6\text{-iPr}_2)_2\}\text{Yb}(\mu\text{-SCH}_2\text{Ph})_2$ ] (2.386(4), 2.408(4) Å),<sup>15b</sup> and [ $\{\text{Cy}_2\text{NC}(\text{NAr}_2)\}\text{Yb}(\mu\text{-I})_2$ ] (2.360(3), 2.424(4) Å).<sup>15a</sup> No other examples of seven-coordinate Yb(II) complexes featuring  $\kappa^1\text{-N}, \eta^6\text{-arene}$  coordination of the amidinate ligand are known so far, limiting possible comparisons. The Yb– $\text{N}_{\text{amide}}$  bond length in 6 (2.368(2) Å) is noticeably shorter than those in seven-coordinate Yb(II)–amide complexes [ $[\text{Na}(\text{THF})]^+[\text{Cp}^*_2\text{YbN}(\text{SiMe}_3)_2]^-$ ] (2.41(2) Å)<sup>16</sup> and [ $\{[(\text{Me}_3\text{Si})_2\text{N}]\text{Yb}(\mu\text{-DAC})\}_2\text{Yb}$ ] (DAC = 4,13-diaza-18-crown-6) (2.43(3)–2.44(3) Å).<sup>17</sup> The Yb– $\text{C}_{\text{arene}}$  distances fall into a rather large range (2.886(2)–3.157(3) Å, average = 3.034(3) Å).<sup>18</sup> The Yb–O coordination bonds in complex 6 have similar lengths: Yb(1A)–O(1A) = 2.483(2) and Yb(1A)–O(1SA) = 2.458(2) Å.

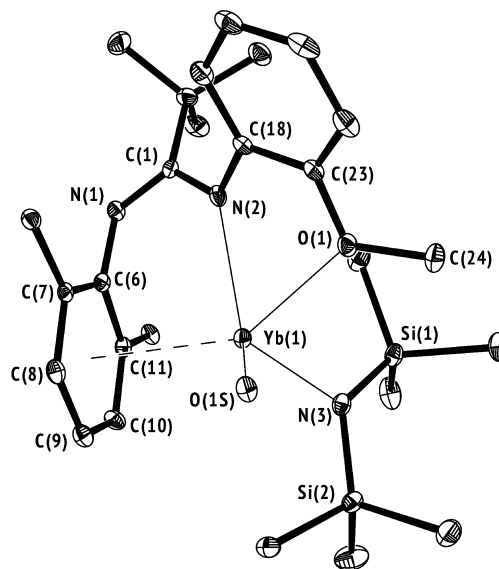


**Figure 1.** Molecular structure of  $[2\text{-MeOC}_6\text{H}_4\text{NC}(t\text{Bu})\text{N}(\text{C}_6\text{H}_3\text{-}i\text{Pr}_2\text{-}2,6)]\text{Yb}[\text{N}(\text{SiMe}_3)_2](\text{THF})$  (6). Only one of the two independent molecules is shown. Hydrogen atoms, methyl fragments of the *iPr* groups, and methylene fragments of the THF molecule are omitted for clarity; thermal ellipsoids drawn at the 30% probability level. Bond lengths (Å) and angles (deg): Yb(1)–N(3) 2.368(2), Yb(1)–N(2) 2.452(2), Yb(1)–O(1S) 2.458(2), Yb(1)–O(1) 2.483(2), Yb(1)–C(6) 2.886(2), Yb(1)–C(7) 2.944(3), Yb(1)–C(8) 3.038(3), Yb(1)–C(11) 3.043(2), Yb(1)–C(9) 3.138(3), Yb(1)–C(10) 3.157(3), Yb(1)–Si(2) 3.4788(8), Yb(1)–Si(1) 3.5501(8), N(1)–C(1) 1.299(3), N(2)–C(1) 1.379(3); N(3)–Yb(1)–N(2) 122.43(7), N(3)–Yb(1)–O(1S) 107.04(7), N(2)–Yb(1)–O(1S) 115.52(7), N(3)–Yb(1)–O(1) 89.75(7), N(2)–Yb(1)–O(1) 64.60(6), O(1S)–Yb(1)–O(1) 78.13(6).

In the  $^1\text{H}$  NMR spectrum of 6 recorded in  $\text{toluene-}d_8$ , the methyl hydrogens of the amidinate isopropyl groups appear as a broadened multiplet at  $\delta$  1.27–1.33 ppm overlapping with the  $\beta\text{-CH}_2$  hydrogens of the THF molecule, and the methine hydrogens of the isopropyl groups give one broad multiplet at  $\delta$  3.46 ppm. The  $\alpha\text{-CH}_2$  THF hydrogens appear as a broadened multiplet at  $\delta$  3.28 ppm. A singlet at  $\delta$  3.51 ppm is assigned to

the methoxy group hydrogens of the amidinate ligand, while the signals arising from the aromatic hydrogens of the 2-methoxyphenyl and 2,6-diisopropylphenyl moieties give rise to a multiplet in the region  $\delta$  6.36–6.80 ppm. The methyl hydrogens of the silylamide ligand appear as a characteristic sharp, high-field shifted singlet at  $\delta$  0.24 ppm. Variable temperature  $^1\text{H}$  and  $^{13}\text{C}$  NMR spectra of complex **6** in the range  $-60$  to  $50$   $^\circ\text{C}$  were recorded in toluene- $d_8$  and THF- $d_8$ ; however, they did not provide informative clues about the actual arene coordination mode in solution, notably if the  $\eta^6$ -coordination observed in the solid state is maintained.

The X-ray diffraction studies of complexes **7** and **8** (Figures 2 and 3) revealed a very unusual  $\pi$ -coordination of the central

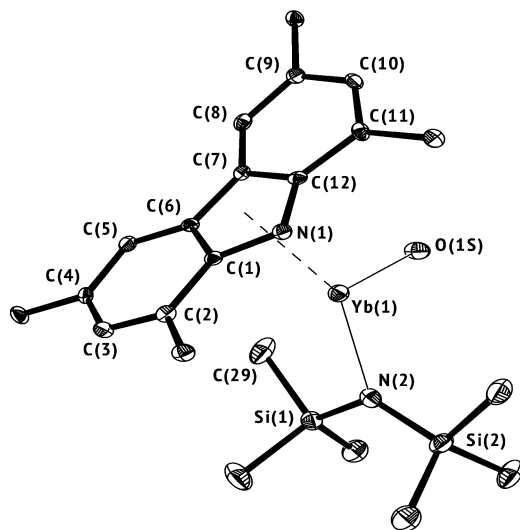


**Figure 2.** Molecular structure of  $[1,3,6,8\text{-}t\text{Bu}_4\text{C}_{12}\text{H}_4\text{N}]\text{Yb}[\text{N}(\text{SiMe}_3)_2](\text{THF})$  (**7**). Hydrogen atoms, methyl fragments of the *t*Bu groups, and methylene fragments of the THF molecule are omitted for clarity; thermal ellipsoids drawn at the 30% probability level. Bond lengths ( $\text{\AA}$ ) and angles ( $^\circ$ ): Yb(1)–N(1) 2.490(3), Yb(1)–N(2) 2.289(3), Yb(1)–O(1S) 2.368(3), Yb(1)–C(1) 2.678(4), Yb(1)–C(6) 2.985(3), Yb(1)–C(7) 3.047(3), Yb(1)–C(12) 2.708(3); N(1)–C(1) 1.373(5), N(1)–C(12) 1.386(5), C(1)–C(6) 1.434(5), C(6)–C(7) 1.431(5), C(7)–C(12) 1.435(5); N(1)–Yb(1)–N(2) 130.2(1), N(1)–Yb(1)–O(1S) 125.2(1), N(2)–Yb(1)–O(1S) 99.1(1), Si(1)–N(2)–Si(2) 128.2(2), Si(1)–N(2)–Yb(1) 103.9(2), Si(2)–N(2)–Yb(1) 128.0(2), carbazole<sub>Centr</sub>–Yb(1)–N(2) 145.9(3).

five-membered ring of 1,3,6,8-tetra-*tert*-butylcarbazol-9-yl ligands to the Yb(II) centers. Unlike lanthanide complexes of unsubstituted<sup>19</sup> or 1,8-disubstituted<sup>20</sup> carbazol-9-yl ligands that feature metal–ligand  $\sigma$ -interaction through the amide *N*-donor, the ytterbium atoms in **7** and **8** are disposed above the pyrrolyl ring (Yb–centroid distances = 2.517(8)  $\text{\AA}$  in **7** and 2.545(7)  $\text{\AA}$  in **8**).<sup>21</sup> Along the Yb–N<sub>Carbazole</sub> bonds (**7**, 2.490(3); **8**, 2.631(3)  $\text{\AA}$ ), bonding of the ytterbium center with two neighboring pyrrolyl carbons are detected in both complexes. The lengths of these two Yb–C bonds (**7**, 2.678(4) and 2.708(3)  $\text{\AA}$ ; **8**, 2.706(4) and 2.840(4)  $\text{\AA}$ ) are comparable to those observed in related Yb(II) cyclopentadienyl complexes [for comparison, see  $\{(\text{C}_5\text{Me}_5)\text{Yb}[\mu\text{-N}(\text{SiMe}_3)_2]\}_2$ : Yb–C<sub>average</sub> = 2.75(2)  $\text{\AA}$ ;<sup>22</sup>  $(\text{C}_5\text{Me}_5)\text{Yb}[\text{N}(\text{SiMe}_3)_2](\text{THF})_2$ , Yb–C = 2.675(4)–2.727(4)  $\text{\AA}$ ].<sup>23</sup> Moreover, two somewhat longer contacts between the ytterbium center and the two remaining distal carbons of the pyrrolyl ring are detected (**7**, 2.985(3) and 3.047(3)  $\text{\AA}$ ; **8**, 2.899(4) and 2.979(4)  $\text{\AA}$ ). These distances are

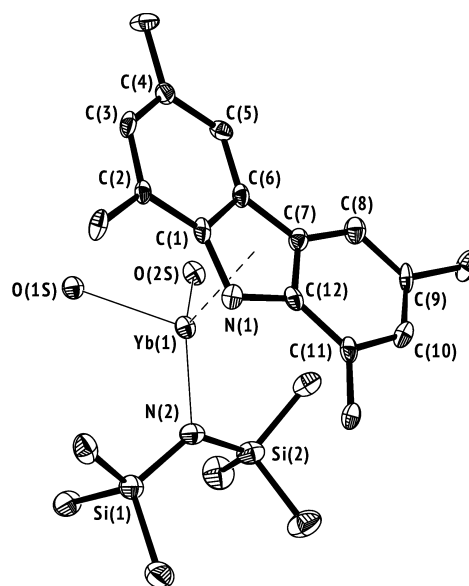


**Figure 3.** Molecular structure of  $[1,3,6,8\text{-}t\text{Bu}_4\text{C}_{12}\text{H}_4\text{N}]\text{Yb}[\text{N}(\text{SiMe}_3)_2](\text{THF})_2$  (**8**). Hydrogen atoms, methyl fragments of the *t*Bu groups, and methylene fragments of the THF molecules are omitted for clarity; thermal ellipsoids drawn at the 30% probability level. Bond lengths ( $\text{\AA}$ ) and angles ( $^\circ$ ): Yb(1)–N(1) 2.631(3), Yb(1)–N(2) 2.323(3), Yb(1)–C(1) 2.706(4), Yb(1)–C(6) 2.899(4), Yb(1)–C(7) 2.979(4), Yb(1)–C(12) 2.840(4), Yb(1)–O(1) 2.428(3), Yb(1)–O(2) 2.407(3), N(1)–Yb(1)–N(2) 121.3(1), N(2)–Yb(1)–O(1) 95.9(1), N(2)–Yb(1)–O(2) 107.2(1), carbazole<sub>Centr</sub>–Yb(1)–N(2) 136.8(4).

just slightly longer than the analogous Yb–C bonds in the bis(fluorenyl)-ytterbium complex  $(\text{C}_{13}\text{H}_9)_2\text{Yb}(\text{THF})_2$  (2.852(7)–2.952(7)  $\text{\AA}$ ).<sup>24</sup> Curiously, the difference of coordination numbers of the metal centers in **7** and **8** does not affect much the Yb–C distances (average Yb–C bond length: **7**, 2.854(3); **8**, 2.856(4)  $\text{\AA}$ ) while, at the same time, the Yb–N<sub>Carbazole</sub> distance in **8** (2.631(3)  $\text{\AA}$ ) is substantially longer than in **7** (2.490(3)  $\text{\AA}$ ). Overall the geometric parameters of complexes **7** and **8** suggest  $\eta^5$ -coordination of the 1,3,6,8-tetra-*tert*-butylcarbazol-9-yl ligands with a noticeable tilting toward the  $\eta^3$ -fashion, as observed in  $(\text{C}_{13}\text{H}_9)_2\text{Ln}(\text{THF})_2$  (Ln = Sm, Yb) complexes.<sup>24,25</sup> The Yb–N<sub>Amido</sub> bond lengths in **7** and **8** (2.289(3) and 2.323(3)  $\text{\AA}$ , respectively) fall in the range of values normally measured in Yb(II) complexes with terminal N(SiMe<sub>3</sub>)<sub>2</sub> ligands.<sup>13,17,26</sup> In complex **7**, the short contacts Yb(1)–Si(1) (3.1465(11)  $\text{\AA}$ ) and Yb(1)–C(29) (2.841(4)  $\text{\AA}$ ), together with noticeable distortion of the geometry around the nitrogen (Si(1)–N(2)–Yb(1), 103.9(2) $^\circ$ , and Si(2)–N(2)–Yb(1), 128.0(2) $^\circ$ ) and silicon (C(29)–Si(1)–N(2), 107.5(2) $^\circ$ ) atoms are indicative of an agostic interaction between the metal center and one of the methyl groups of the silylamide ligand.<sup>27</sup> In complex **8**, which contains a more coordinatively saturated Yb(II) center, no such agostic interaction was observed.

In the  $^1\text{H}$  NMR spectrum of **7** recorded in  $\text{C}_6\text{D}_6$  solution at ambient temperature, the *t*Bu groups of the carbazolyl ligand give rise to a slightly broadened singlet at  $\delta$  1.48 ppm; the aromatic hydrogens of the carbazolyl moiety appear as two doublets at  $\delta$  7.59 and 8.23 ppm ( $^4J_{\text{H-H}} = 1.4$  Hz). A sharp, high-field shifted singlet at  $\delta$  0.37 ppm corresponds to the silylamide ligand. The hydrogens of the THF molecule give two slightly broadened singlets at  $\delta$  1.27 and 3.53 ppm. The  $^1\text{H}$



NMR spectrum of **8** is similar to that of **7** with the only difference being the integral intensity of the signals corresponding to the THF hydrogens.

**Hydrophosphination Catalysis.** Ytterbium(II) complexes **5–7** were investigated as catalyst precursors in the hydrophosphination reaction between styrene and  $\text{Ph}_2\text{PH}$  or  $\text{PhPH}_2$ , chosen as model reactions. Representative results are reported in Table 1. All reactions were found to be regioselective,

**Table 1.** Hydrophosphination of Styrene with  $\text{Ph}_2\text{PH}$  and  $\text{PhPH}_2$  Catalyzed by Yb(II)–Amide Complexes **5–7**<sup>a</sup>

R = Ph, H

entry	complex [mol %]	phosphine	time [h]	conversion [%]
1	<b>5</b> (2.0)	$\text{Ph}_2\text{PH}$	0.25	27
2	<b>5</b> (2.0)	$\text{Ph}_2\text{PH}$	2	55
3	<b>6</b> (2.0)	$\text{Ph}_2\text{PH}$	0.25	17
4	<b>6</b> (2.0)	$\text{Ph}_2\text{PH}$	2	27
5	<b>7</b> (2.0)	$\text{Ph}_2\text{PH}$	0.25	31
6	<b>7</b> (2.0)	$\text{Ph}_2\text{PH}$	2	71
7	<b>7</b> (1.0)	$\text{Ph}_2\text{PH}$	4	92
8	<b>7</b> (0.5)	$\text{Ph}_2\text{PH}$	8	15
9	<b>7</b> (2.0)	$\text{PhPH}_2$	10	30
10	<b>7</b> (2.0)	$\text{PhPH}_2$	60	61
11	$[(\text{Me}_3\text{Si})_2\text{N}]_2\text{Yb}(\text{THF})_2$ (2.0)	$\text{Ph}_2\text{PH}$	2	24

<sup>a</sup>Reaction conditions: neat substrates in a 1:1 ratio, 60 °C. Conversion determined by  $^1\text{H}$  NMR spectroscopy in  $\text{C}_6\text{D}_6$ .

forming exclusively the anti-Markovnikov addition product. Complex **7** was found to be the most productive over the series (compare entries 2, 4, and 6), although all three complexes featured performance of the same magnitude. The catalytic activity of **5–7** in the hydrophosphination of styrene with diphenylphosphine, especially that of **7**, is remarkable and is commensurate to that which we recently disclosed for an Yb(II)–amide complex supported by an anilido–imine ligand.<sup>28</sup> Notably, the performance of **5** and **7** is clearly superior to that of the simple precursor  $[(\text{Me}_3\text{Si})_2\text{N}]_2\text{Yb}(\text{THF})_2$  (entry 11). The reactivity of phenylphosphine with **7** proved considerably lower than that of diphenylphosphine (entries 9–10). Of note, only the primary hydrophosphination product was formed in the latter reactions with  $\text{PhPH}_2$ ; i.e., no  $(\text{PhCH}_2\text{CH}_2)_2\text{PPh}$  eventually resulting from subsequent reaction of  $\text{PhCH}_2\text{CH}_2\text{PPh}$  with styrene was observed.

Besides experiments using 50 equiv of styrene and  $\text{Ph}_2\text{PH}$ , the limit of complex **7** was evaluated by increasing the substrates loading up to 100 and 200 equiv (with  $[\text{styrene}]/[\text{Ph}_2\text{PH}] = 1:1$ ). The neat reaction using 100 equiv of substrates reached 92% conversion after 4 h at 60 °C. However, in the presence of 200 equiv of substrates, only 15% conversion was observed after 8 h, suggesting catalyst decay. Actually, in the experiments performed over 2 h at such low catalyst loadings, we noticed that the color of the solution gradually changed from deep red to pale yellow; this is consistent with an oxidation of Yb(II) to Yb(III). This hypothesis is also corroborated by the observation of broad resonances in all NMR spectra of the crude reaction mixtures, diagnostic of

paramagnetic Yb(III) species, especially at high styrene concentrations.<sup>29</sup> This putative oxidation of divalent ytterbium with styrene, in the presence of phosphine (or amine, *vide infra*), is reminiscent of our recent results with related divalent lanthanide systems.<sup>28</sup>

More detailed kinetic data about this reaction were sought after using **7** as a precatalyst, with relatively large catalyst loadings (>6.6 mol-%) to prevent as much as possible problems connected to the above-mentioned catalyst decay. To determine the partial order in  $\text{Ph}_2\text{PH}$ , its conversion over time was studied using a large excess of styrene, at three different  $[\text{phosphine}]/[\text{7}]$  ratios (see the Supporting Information, Figures S6–S8). In all cases, similar values of  $k_{\text{app}}$  were obtained ( $0.107\text{ s}^{-1}$ ,  $0.133\text{ s}^{-1}$ , and  $0.125\text{ s}^{-1}$ , that is,  $0.120 \pm 0.013\text{ s}^{-1}$ ), thus suggesting a zeroth order dependence on phosphine. Another interesting observation in these experiments is the induction period which was observed in all cases. In fact, the larger the amount of  $\text{Ph}_2\text{PH}$ , the shorter the induction period: 3 equiv, 98 s; 7 equiv, 81 s; 15 equiv, 36 s (data obtained by extrapolation of least-squares linear regression laws, see Figures S6–S8). This may suggest that the Yb(II)–amide complex reacts with the phosphine to produce the real catalytic species, tentatively assigned as a Yb(II)– $\text{PPh}_2$  species. Unfortunately, attempts to prepare this putative phosphide species, through independent reactions of  $\text{Ph}_2\text{PH}$  with **7**, have been unsuccessful thus far.

In order to determine the partial order in the catalyst, the conversion of the phosphine was studied using a large excess of styrene at different catalyst concentrations (over a 10-fold range, in the range 6.25–63 mM) while maintaining the total volume of reactants and solvent constant. The apparent rate constants ( $k_{\text{app}}$ ) were thus determined for substrate conversion below 70% (see the Supporting Information Table S1). The plot of  $\ln(k_{\text{app}})$  vs  $\ln([7]_0)$  gave a straight line ( $R^2 = 0.957$ ) with a slope of 0.5 corresponding to the apparent kinetic order for the precatalyst (Figure 4; see also Figure S9).

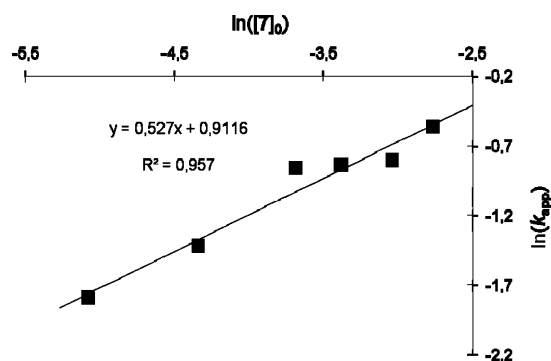


**Figure 4.** Plot of  $\ln(k_{\text{app}})$  vs  $\ln([7]_0)$  for the intermolecular hydrophosphination of styrene and  $\text{Ph}_2\text{PH}$  catalyzed by **7** at different catalyst concentrations (6.25, 13.0, 25.0, 34.0, 47.0, and 63.0 mM). Reaction conditions: 60 °C,  $[\text{styrene}]_0 = 1.34\text{ M}$ ,  $[\text{styrene}]_0/[\text{Ph}_2\text{PH}]_0 = 10:1$ ,  $\text{C}_6\text{D}_6 + \text{Ph}_2\text{PH} + \text{styrene} = 0.6\text{ mL}$ .

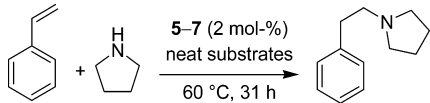
Further experiments were conducted to determine the partial order in styrene, using a constant concentration of the catalyst and the phosphine and varying the concentration of styrene in the reaction mixture in a *ca.* 10-fold range (in the range 0.33–2.61 M).<sup>30</sup> Similar treatment as that performed above gave an apparent partial order in styrene of 0.72 ( $R^2 = 0.985$ ). However, because of the narrow concentration range (due to

experimental constraints),<sup>30</sup> a substantial error exists, and the values are also quite consistent with a partial first-order on styrene ( $R^2 = 0.962$ ; see Figures S10–S12 and Table S2). Since a first order is usually observed for intermolecular hydrophosphination of styrene with group 2 and 3 divalent metals,<sup>11,12,28</sup> we assume this is also the case here.

On the basis of previous results with related Yb(II) catalytic systems,<sup>28</sup> we anticipated to find a zeroth order for Ph<sub>2</sub>PH and a first order for styrene and the catalyst, respectively. In fact, the data with **7** are consistent with a zeroth order in phosphine and a first order in styrene but indicate a 0.5 order for the catalyst, suggesting that the precatalyst (putatively a Yb(II)-phosphide) has a dimeric association in solution or is involved in a reversible dimer–monomer aggregation phenomenon. In order to obtain additional evidence for a dimeric structure of the real catalytic species in solution, the NMR-tube reactions of complexes **5–7** with equimolar amounts of Ph<sub>2</sub>PH (C<sub>6</sub>D<sub>6</sub>, r.t.) were carried out. All the reactions were found to occur with the release of amine and formation of precipitates, albeit the <sup>31</sup>P and <sup>171</sup>Yb spectra of the reaction mixtures turned out to be uninformative. In particular, no coupling patterns were observed in the <sup>31</sup>P and <sup>171</sup>Yb spectra.

**Hydroamination Catalysis.** Complexes **5–7** have been also investigated briefly in the intermolecular hydroamination of styrene and pyrrolidine. Experiments were performed in neat reagents, using a 2 mol loading of the precatalyst at 60 °C. Representative results are reported in Table 2. In all cases, only

**Table 2. Intermolecular Hydroamination of Styrene with Pyrrolidine Promoted by **5–7****



entry	complex [mol %]	time [h]	conv. [%]
1	<b>5</b> (2.0)	31	12
2	<b>6</b> (2.0)	31	85
3	<b>7</b> (2.0)	31	96
4	[(Me <sub>3</sub> Si) <sub>2</sub> N] <sub>2</sub> Yb(THF) <sub>2</sub> (2.0)	31	37

the anti-Markovnikov hydroamination product was observed. As for hydrophosphination reactions, complex **7** proved to be the most productive, with nearly complete conversion after 31 h of reaction, somewhat better than with **6**, and much better than with **5** or the simple precursor [(Me<sub>3</sub>Si)<sub>2</sub>N]<sub>2</sub>Yb(THF)<sub>2</sub>. In fact, with the latter complexes **5** and [(Me<sub>3</sub>Si)<sub>2</sub>N]<sub>2</sub>Yb(THF)<sub>2</sub>, the color of the reaction mixture turned from red to yellow within minutes, indicating rapid catalyst decay (oxidation); in these cases, and in contrast to the hydroamination reactions conducted with **6** and **7** (see Figure S13), the NMR spectra of the crude reaction mixtures featured rather broad resonances, indicating the presence of Yb(III) species; also, formation of an unidentified precipitate was noted when [(Me<sub>3</sub>Si)<sub>2</sub>N]<sub>2</sub>Yb(THF)<sub>2</sub> was used as a catalyst precursor. It is important to note that the yet unidentified species resulting from the oxidation of **5** under the reaction conditions is (are) not active (or at least significantly less than **5**). This provides indirect evidence that the true active species in these hydroelementation reactions are indeed divalent ytterbium species.

The catalytic performance of precatalysts **6** and **7** are remarkable since with another Yb(II)–amide complex supported by an monoanionic anilido–imine ligand,<sup>28</sup> no

hydroamination took place under the same conditions: this complex immediately decomposed (likely oxidized) in the presence of styrene and pyrrolidine (also evidenced by the rapid color change from purple to light yellow concomitant with the formation of a precipitate), and only the starting reagents were observed.<sup>28</sup>

## CONCLUSIONS

The amine elimination reactions of [(Me<sub>3</sub>Si)<sub>2</sub>N]<sub>2</sub>Yb(THF)<sub>2</sub> with amidine 2-MeOC<sub>6</sub>H<sub>4</sub>NHC(tBu)=N(C<sub>6</sub>H<sub>3</sub>-iPr<sub>2</sub>-2,6) and 1,3,6,8-tetra-*tert*-butylcarbazol pro-ligands allowed for the synthesis of new heteroleptic Yb(II) amido complexes which were isolated in high yields. The solid state structures of complexes **6–8** revealed profound changes of coordination modes of conventional ligands provoked by modification of their denticity and steric bulkiness. The introduction of an additional Lewis base group (i.e., OMe) into one of the aryl substituents of the amidinate ligand leads to an unprecedented  $\kappa^1$ -N, $\kappa^2$ -O, $\eta^6$ -arene coordination, instead of the classic  $\kappa^2$ -N,N' mode. Similarly, replacing a simple carbazol-9-yl by 1,3,6,8-tetra-*tert*-butylcarbazol-9-yl ligand results in the switch of coordination mode from  $\sigma$  to  $\pi$ .

The Yb(II)–amide complexes **5–7** all proved able to promote intermolecular hydroelementation of styrene under mild conditions; however, their catalytic performances are quite contrasted. The carbazol-9-yl-Yb(II)–amide revealed superior abilities for both hydrophosphination and hydroamination, as compared to amidinates **5** and **6**. This can be tentatively related to the lower (formal) coordination number of complex **7**, as in this type of catalysis, activity tends to increase when the C.N. of the catalyst decreases. The high activity of complex **7** in hydrophosphination is commensurate to that of a recently reported {anilido-imine}Yb(II)–amide,<sup>28</sup> but it is remarkable that it also promotes efficiently the addition of pyrrolidine onto styrene, while the {anilido-imine}Yb(II)–amide proved completely unable to do so, due to rapid decomposition/oxidation in the presence of these reagents. This clearly evidences that the reactivity and stability of those classes of divalent lanthanide complexes can be largely tuned with appropriate ligand frameworks. Research along these lines is currently under progress in our laboratories.

## EXPERIMENTAL SECTION

**General Considerations.** All experiments were performed in evacuated tubes, using standard Schlenk-flask or glovebox techniques, with rigorous exclusion of traces of moisture and air. After drying over KOH, THF and DME were purified by distillation from sodium/benzophenone ketyl, hexane, and toluene by distillation from sodium/triglyme benzophenone ketyl prior to use. C<sub>6</sub>D<sub>6</sub> toluene-*d*<sub>8</sub> and THF-*d*<sub>8</sub> were dried with sodium/benzophenone ketyl and condensed in a vacuum prior to use. Yb[N(SiMe<sub>3</sub>)<sub>2</sub>]<sub>2</sub>(THF)<sub>2</sub> was prepared according to literature procedures.<sup>13</sup> PhSiH<sub>3</sub> was purchased from Aldrich and was dried over CaH<sub>2</sub> and condensed in a vacuum prior to use. (PhCH<sub>2</sub>S)<sub>2</sub> and Ph<sub>3</sub>SnCl were purchased from Acros and were used without additional purification. Styrene and pyrrolidine were purchased from Aldrich or Acros and were vacuum-distilled over CaH<sub>2</sub> and then were degassed by freeze–pump–thaw methods. Diphenylphosphine and phenylphosphine were purchased from Aldrich and used as received.

**Instruments and Measurements.** NMR spectra were recorded on a Bruker DPX 200 or Bruker Avance DRX-400 spectrometer. Chemical shifts for <sup>1</sup>H and <sup>13</sup>C{<sup>1</sup>H} spectra were referenced internally using the residual solvent resonances and are reported relative to TMS. Lanthanide metal analysis was carried out by complexometric

Table 3. Crystallographic Data and Structure Refinement Details for 6–8

	6	7	8
formula	C <sub>34</sub> H <sub>59</sub> N <sub>3</sub> O <sub>2</sub> Si <sub>2</sub> Yb	C <sub>38</sub> H <sub>66</sub> N <sub>2</sub> O <sub>2</sub> Si <sub>2</sub> Yb	C <sub>46</sub> H <sub>82</sub> N <sub>2</sub> O <sub>3</sub> Si <sub>2</sub> Yb
<i>M<sub>r</sub></i>	771.06	796.15	940.36
cryst size, mm	0.19 × 0.15 × 0.09	0.23 × 0.14 × 0.11	0.28 × 0.10 × 0.08
cryst syst	triclinic	orthorhombic	orthorhombic
space group	<i>P</i> $\bar{1}$	<i>P</i> 2(1)2(1)2(1)	<i>Pha</i> 2(1)
<i>a</i> , Å	10.3636(6)	9.3830(3)	18.663(1)
<i>b</i> , Å	17.943(1)	12.5151(5)	24.031(2)
<i>c</i> , Å	20.441(1)	34.574(1)	10.9921(8)
$\alpha$ , deg	79.836(2)	90	90
$\beta$ , deg	88.185(2)	90	90
$\gamma$ , deg	87.923(2)	90	90
cell volume, Å <sup>3</sup>	3737.7(4)	4060.0(3)	4929.8(6)
<i>Z</i>	4	4	4
<i>D</i> <sub>calc</sub> , g/cm <sup>3</sup>	1.370	1.302	1.267
$\mu$ , mm <sup>−1</sup>	2.598	2.391	1.983
<i>F</i> <sub>000</sub>	1592	1656	1976
2 $\theta$ range, °	54	54	52
index ranges	−13 ≤ <i>h</i> ≤ 13 −22 ≤ <i>k</i> ≤ 22 0 ≤ <i>l</i> ≤ 26	−11 ≤ <i>h</i> ≤ 11 −15 ≤ <i>k</i> ≤ 15 −44 ≤ <i>l</i> ≤ 43	−23 ≤ <i>h</i> ≤ 23 −29 ≤ <i>k</i> ≤ 29 −13 ≤ <i>l</i> ≤ 13
reflns collected		37676	41419
independent reflns	26106	8796	9682
<i>R</i> <sub>int</sub>		0.0646	0.0809
completeness to $\theta$	98.5	99.4	99.9
data/restraints/params	26106/0/786	8796/1/403	9682/22/518
GoF	1.010	1.039	0.978
<i>R</i> <sub>1</sub> ( <i>I</i> > 2 $\sigma$ ( <i>I</i> ))	0.0298	0.0356	0.0414
<i>wR</i> <sub>2</sub> (all data)	0.0674	0.0749	0.0778
max. and min transmission	0.7998/0.6381	0.7789/0.6093	0.8575/0.6067
absolute structure parameter			−0.019(9)
largest diff. peak and hole, e/Å <sup>3</sup>	2.063/−0.948	1.428/−0.567	1.056/−0.785

titration.<sup>31</sup> C, H, and N elemental combustion analysis was performed in the microanalytical laboratory of IOMC.

[2-MeOC<sub>6</sub>H<sub>4</sub>NC(tBu)N(C<sub>6</sub>H<sub>3</sub>-iPr<sub>2</sub>-2,6)]YbN(SiMe<sub>3</sub>)<sub>2</sub>(THF) (6). A solution of 2-MeOC<sub>6</sub>H<sub>4</sub>NHC(tBu)=N(C<sub>6</sub>H<sub>3</sub>-iPr<sub>2</sub>-2,6) (0.360 g, 0.98 mmol) in toluene (10 mL) was added to a solution of [(Me<sub>3</sub>Si)<sub>2</sub>N]<sub>2</sub>Yb(THF)<sub>2</sub> (0.628 g, 0.98 mmol) in toluene (10 mL) at room temperature. The reaction mixture was stirred for 1 h, and then volatiles were removed in a vacuum. The solid residue was dissolved in hexane (40 mL), and the resulting solution was centrifuged. Slow concentration of the hexane solution at room temperature resulted in the formation of complex 6 as dark red crystals. The mother liquid was decanted, and the crystals were washed with cold hexane and dried in a vacuum for 30 min. Complex 2 was isolated in 78% yield (0.588 g, 0.76 mmol). <sup>1</sup>H NMR (400 MHz, C<sub>7</sub>D<sub>8</sub>, 293 K):  $\delta$  0.24 (s, 18H, SiMe<sub>3</sub>), 1.27–1.33 (complex m, 16H, CH<sub>3</sub> iPr and  $\beta$ -CH<sub>2</sub> THF), 1.65 (s, 9H, CH<sub>3</sub> tBu), 3.28 (br s, 4H,  $\alpha$ -CH<sub>2</sub> THF), 3.46 (br m, 2H, CH iPr), 3.51 (s, 3H, OMe), 6.36 (br d, <sup>3</sup>*J*<sub>HH</sub> = 7.3 Hz, 1H, CH C<sub>6</sub>H<sub>4</sub>OMe), 6.50 (complex m, 2H, CH C<sub>6</sub>H<sub>4</sub>OMe), 6.80 (complex m, 4H, CH C<sub>6</sub>H<sub>4</sub>OMe and C<sub>6</sub>H<sub>3</sub>iPr<sub>2</sub>) ppm. <sup>13</sup>C{<sup>1</sup>H} NMR (100 MHz, C<sub>7</sub>D<sub>8</sub>, 293 K):  $\delta$  5.7 (s, SiMe<sub>3</sub>), 21.2 (s, CH<sub>3</sub> iPr), 21.5 (s, CH<sub>3</sub> iPr), 23.4 (s, CH<sub>3</sub> iPr), 24.9 (s,  $\beta$ -CH<sub>2</sub> THF), 28.3 (s, CH<sub>3</sub> iPr), 28.4 (s, CH iPr), 29.1 (s, CH iPr), 31.7 (s, CH<sub>3</sub> tBu), 41.1 (s, C tBu), 56.4 (s, CH<sub>3</sub> OMe), 68.6 (s,  $\alpha$ -CH<sub>2</sub> THF), 110.4 (s, CH C<sub>6</sub>H<sub>4</sub>OMe), 115.9 (s, CH C<sub>6</sub>H<sub>4</sub>OMe), 120.3 (s, CH C<sub>6</sub>H<sub>4</sub>OMe), 121.9 (s, CH C<sub>6</sub>H<sub>3</sub>iPr<sub>2</sub>), 122.6 (s, CH C<sub>6</sub>H<sub>4</sub>OMe), 123.3 (s, CH C<sub>6</sub>H<sub>3</sub>iPr<sub>2</sub>), 123.6 (s, CH C<sub>6</sub>H<sub>3</sub>iPr<sub>2</sub>), 136.8 (s, C *ipso*-NC<sub>6</sub>H<sub>4</sub>OMe), 140.6 (s, C *ortho*-NC<sub>6</sub>H<sub>3</sub>iPr<sub>2</sub>), 142.6 (s, C *ortho*-NC<sub>6</sub>H<sub>3</sub>iPr<sub>2</sub>), 147.4 (s, C *ortho*-NC<sub>6</sub>H<sub>4</sub>OMe), 154.2 (s, C *ipso*-NC<sub>6</sub>H<sub>3</sub>iPr<sub>2</sub>), 174.0 (s, C N=C=N) ppm. Elem. anal. calcd for C<sub>34</sub>H<sub>59</sub>N<sub>3</sub>O<sub>2</sub>Si<sub>2</sub>Yb (771.08 g/mol): C, 52.96; H, 7.71; N, 5.45; Yb, 22.44. Found: C, 53.34; H, 7.53; N, 5.89; Yb, 22.70.

[1,3,6,8-tBu<sub>4</sub>C<sub>12</sub>H<sub>4</sub>N]Yb[N(SiMe<sub>3</sub>)<sub>2</sub>](THF) (7). A solution of 1,3,6,8-tBu<sub>4</sub>C<sub>12</sub>H<sub>4</sub>NH (0.502 g, 1.29 mmol) in toluene (10 mL) was added to a solution of [(Me<sub>3</sub>Si)<sub>2</sub>N]<sub>2</sub>Yb(THF)<sub>2</sub> (0.820 g, 1.29 mmol) in toluene (15 mL) at room temperature. The reaction mixture was stirred at 70 °C for 3 days, volatiles were removed in a vacuum, the solid residue was dissolved in hexane (20 mL), and the resulting solution was centrifuged. Slow concentration of the hexane solution at room temperature and prolonged cooling of the concentrated solution at −30 °C resulted in the formation of complex 7 as bright orange crystals. The mother liquid was decanted, and the crystals were washed with cold hexane and dried in a vacuum for 30 min. Complex 7 was isolated in 90% yield (0.921 g, 1.16 mmol). <sup>1</sup>H NMR (400 MHz, C<sub>7</sub>D<sub>8</sub>, 293 K):  $\delta$  0.37 (s, 18H, SiMe<sub>3</sub>), 1.27 (br m, 4H,  $\beta$ -CH<sub>2</sub> THF), 1.48 (s, 36H, CH<sub>3</sub> tBu), 3.53 (br m, 4H,  $\alpha$ -CH<sub>2</sub> THF), 7.59 (d, <sup>4</sup>*J*<sub>HH</sub> = 1.4 Hz, 2H, CH C<sub>12</sub>H<sub>4</sub>N), 8.23 (d, <sup>4</sup>*J*<sub>HH</sub> = 1.4 Hz, 2H, CH C<sub>12</sub>H<sub>4</sub>N) ppm. <sup>13</sup>C{<sup>1</sup>H} NMR (100 MHz, C<sub>7</sub>D<sub>8</sub>, 293 K):  $\delta$  5.3 (s, SiMe<sub>3</sub>), 24.7 (s,  $\beta$ -CH<sub>2</sub> THF), 30.1 (s, CH<sub>3</sub> tBu), 31.9 (s, CH<sub>3</sub> tBu), 34.4 (s, C tBu), 34.7 (s, C tBu), 69.3 (s,  $\alpha$ -CH<sub>2</sub> THF), 114.3 (s, CH C<sub>12</sub>H<sub>4</sub>N), 120.0 (s, CH C<sub>12</sub>H<sub>4</sub>N), 124.6 (s, C C<sub>12</sub>H<sub>4</sub>N), 131.7 (s, C C<sub>12</sub>H<sub>4</sub>N), 135.6 (s, C C<sub>12</sub>H<sub>4</sub>N), 1420 (s, C C<sub>12</sub>H<sub>4</sub>N) ppm. Elem. anal. calcd for C<sub>38</sub>H<sub>66</sub>N<sub>2</sub>O<sub>2</sub>Si<sub>2</sub>Yb (796.17 g/mol): C, 57.33; H, 8.36; N, 3.52; Yb, 21.74. Found: C, 57.68; H, 8.70; N, 3.29; Yb, 21.90.

[1,3,6,8-tBu<sub>4</sub>C<sub>12</sub>H<sub>4</sub>N]Yb[N(SiMe<sub>3</sub>)<sub>2</sub>](THF)<sub>2</sub> (8). A solution of 1,3,6,8-tBu<sub>4</sub>C<sub>12</sub>H<sub>4</sub>NH (0.550 g, 1.41 mmol) in toluene (10 mL) was added to a solution of [(Me<sub>3</sub>Si)<sub>2</sub>N]<sub>2</sub>Yb(THF)<sub>2</sub> (0.899 g, 1.41 mmol) in toluene (15 mL) at room temperature. The reaction mixture was stirred at 70 °C for 3 days, and volatiles were then removed in a vacuum. Complex 8 was obtained after recrystallization of the solid reaction products from a toluene/THF (10:1) mixture by slow concentration at room temperature as bright orange cubic crystals. The mother liquid was decanted, and the crystals were washed with a small amount of cold



hexane. Complex **8** was isolated in 85% yield (1.040 g, 1.20 mmol).  $^1\text{H}$  NMR (400 MHz,  $\text{C}_7\text{D}_8$ , 293 K):  $\delta$  0.37 (s, 18H,  $\text{SiMe}_3$ ), 1.27 (br m, 8H,  $\beta\text{-CH}_2$ , THF), 1.48 (s, 36H,  $\text{CH}_3$  tBu), 3.53 (br m, 8H,  $\alpha\text{-CH}_2$ , THF), 7.59 (d,  $^4J_{\text{HH}} = 1.4$  Hz, 2H,  $\text{CH}$   $\text{C}_{12}\text{H}_4\text{N}$ ), 8.23 (d,  $^4J_{\text{HH}} = 1.4$  Hz, 2H,  $\text{CH}$   $\text{C}_{12}\text{H}_4\text{N}$ ) ppm.  $^{13}\text{C}\{^1\text{H}\}$  NMR (100 MHz,  $\text{C}_7\text{D}_8$ , 293 K):  $\delta$  5.3 (s,  $\text{SiMe}_3$ ), 24.7 (s,  $\beta\text{-CH}_2$ , THF), 30.1 (s,  $\text{CH}_3$  tBu), 31.9 (s,  $\text{CH}_3$  tBu), 34.4 (s,  $\text{C}$  tBu), 34.7 (s,  $\text{C}$  tBu), 69.3 (s,  $\alpha\text{-CH}_2$ , THF), 114.3 (s,  $\text{CH}$   $\text{C}_{12}\text{H}_4\text{N}$ ), 120.0 (s,  $\text{CH}$   $\text{C}_{12}\text{H}_4\text{N}$ ), 124.6 (s,  $\text{C}$   $\text{C}_{12}\text{H}_4\text{N}$ ), 131.7 (s,  $\text{C}$   $\text{C}_{12}\text{H}_4\text{N}$ ), 135.6 (s,  $\text{C}$   $\text{C}_{12}\text{H}_4\text{N}$ ), 1420 (s,  $\text{C}$   $\text{C}_{12}\text{H}_4\text{N}$ ) ppm. Elem. anal. calcd for  $\text{C}_{42}\text{H}_{74}\text{N}_2\text{O}_2\text{Si}_2\text{Yb}$  (868.27 g/mol): C, 58.10; H, 8.59; N, 3.23; Yb, 19.93. Found: C, 58.18; H, 8.70; N, 3.29; Yb, 19.90.

**Hydrophosphination/Hydroamination Experiments.** In a typical hydrophosphination experiment, the complex was loaded in an NMR tube in the glovebox. Styrene and  $\text{Ph}_2\text{PH}$  were then added in and the reaction time started after heating the NMR tube at 60 °C in a preheated oil bath. After the desired reaction time,  $\text{C}_6\text{D}_6$  was added to the reaction mixture, and the  $^1\text{H}$  NMR spectrum was recorded shortly after at regular time intervals. Conversion was determined by integrating the remaining styrene and the newly formed addition product.

**X-Ray Crystallography.** The X-ray data for **6–8** were collected on a Smart Apex diffractometer (graphite monochromated, MoK $\alpha$  radiation,  $\omega$ -scan technique,  $\lambda = 0.71073$  Å,  $T = 100(2)$  K). The structures were solved by direct methods and were refined on  $F^2$  using the SHELXTL package.<sup>32</sup> All non-hydrogen atoms were found from Fourier syntheses of electron density and were refined anisotropically. All hydrogen atoms were placed in calculated positions and were refined in the riding model. SADABS<sup>33</sup> was used to perform area-detector scaling and absorption corrections. The X-ray data for complex **6** were refined using the HKLF5 method. The details of crystallographic, collection, and refinement data are shown in Table 3, and corresponding CIF files are available as Supporting Information. CCDC-969365 (**6**), -969366 (**7**), and -969367 (**8**) contain the supplementary crystallographic data for this paper. These data can be obtained free of charge from The Cambridge Crystallographic Data Centre via [ccdc.cam.ac.uk/products/csd/request](http://ccdc.cam.ac.uk/products/csd/request).

## ■ ASSOCIATED CONTENT

### ■ Supporting Information

Representative  $^1\text{H}$  and  $^{13}\text{C}$  NMR spectra of ytterbium complexes; crystallographic data for **6**, **7**, and **8** as CIF files; and representative NMR spectra and kinetic monitoring for hydrophosphination reactions. This material is available free of charge via the Internet at <http://pubs.acs.org>

## ■ AUTHOR INFORMATION

### Corresponding Authors

\*Fax: (+33)(0)2 23 23 6939. E-mail: [jean-francois.carpentier@univ-rennes1.fr](mailto:jean-francois.carpentier@univ-rennes1.fr).

\*Fax: (+7)8314621497. E-mail: [trif@iomc.ras.ru](mailto:trif@iomc.ras.ru).

### Notes

The authors declare no competing financial interest.

## ■ ACKNOWLEDGMENTS

The study was supported the Russian Foundation for Basic Research (12-03-93109-HUHNII\_a), Program of the Presidium of the Russian Academy of Science (RAS), RAS Chemistry and Material Science Division, and the French ANR GreenLAKE project (grant ANR-11-BS07-009-01 to SCR). The authors also thank the Groupe de Recherche International (GDRI) CNRS-RAS “Homogeneous Catalysis for Sustainable Development” for support.

## ■ REFERENCES

- (1) (a) Hou, Z.; Wakatsuki, Y. *Coord. Chem. Rev.* **2002**, 231, 1–22. (b) Nakayama, Y.; Yasuda, H. *J. Organomet. Chem.* **2004**, 689, 4489–4511. (c) Gromada, J.; Carpentier, J.-F.; Mortreux, A. *Coord. Chem. Rev.* **2004**, 248, 397–410.
- (2) (a) Jeske, G.; Lauke, H.; Mauermann, H.; Swepston, P. N.; Schumann, H.; Marks, T. J. *J. Am. Chem. Soc.* **1985**, 107, 8091–8103. (b) Jeske, G.; Schock, L. E.; Swepston, P. N.; Schumann, H.; Marks, T. J. *J. Am. Chem. Soc.* **1985**, 107, 8103–8110.
- (3) Molander, G. A.; Romero, J. A. *C. Chem. Rev.* **2002**, 102, 2161–2185.
- (4) (a) Hong, S.; Marks, T. J. *Adv. Chem. Res.* **2004**, 37, 673. (b) Müller, T. E.; Hultsch, K. C.; Yus, M.; Foubelo, F.; Tada, M. *Chem. Rev.* **2008**, 108, 3795–3892. (c) Hultsch, K. C. *Adv. Synth. Catal.* **2005**, 347, 367–391.
- (5) (a) Kawaoka, A.; Marks, T. J. *J. Am. Chem. Soc.* **2005**, 127, 6311–6324. (b) Kawaoka, A. M.; Marks, T. J. *J. Am. Chem. Soc.* **2004**, 126, 12764–12765. (c) Kawaoka, A. M.; Douglass, M. R.; Marks, T. J. *Organometallics* **2003**, 22, 4030–4032. (d) Douglass, M. R.; Stern, C. L.; Marks, T. J. *J. Am. Chem. Soc.* **2001**, 123, 10221–10238. (e) Douglass, M. R.; Marks, T. J. *J. Am. Chem. Soc.* **2000**, 122, 1824–1825. (f) Motta, A.; Fragala, I. L.; Marks, T. J. *Organometallics* **2005**, 24, 4995–5003.
- (6) Weiss, C. J.; Marks, T. J. *Dalton Trans.* **2010**, 39, 6576–6588.
- (7) (a) Harrison, K. N.; Marks, T. J. *J. Am. Chem. Soc.* **1992**, 114, 9220. (b) Bijpost, E. A.; Duchateau, R.; Teuben, J. H. *J. Mol. Catal. A* **1995**, 95, 121.
- (8) (a) Harder, S. *Angew. Chem., Int. Ed.* **2004**, 43, 2714–2718. (b) Ruspic, C.; Spielmann, J.; Harder, S. *Inorg. Chem.* **2007**, 46, 5320–5326. (c) Collin, J.; Giuseppone, N.; Van de Weghe, P. *Coord. Chem. Rev.* **1998**, 117–144, 178–180. (d) Yasuda, H.; Ihara, E.; Hayakawa, T.; Kakehi, T.; Macromol, J. *Sci. Pure Appl. Chem.* **1997**, A34 (10), 1929–1944. (e) Schmid, M.; Guillaume, S. M.; Roesky, P. W. *J. Organomet. Chem.* **2013**, 744, 68–73. (f) Korobkov, I.; Gambarotta, S. *Organometallics* **2009**, 28, 4009–4019.
- (9) Shannon, R. D. *Acta Crystallogr.* **1976**, 32, 751–767.
- (10) Morss, L. R. *Chem. Rev.* **1976**, 76, 827–841.
- (11) (a) Li, Y. G.; Marks, T. J. *Organometallics* **1996**, 15, 3770–3772. (b) Ryu, J.-S.; Li, Y. G.; Marks, T. J. *J. Am. Chem. Soc.* **2003**, 125, 12584–12605.
- (12) (a) Crimin, M. R.; Barrett, A. G. M.; Hill, M. S.; Hitchcock, P. B.; Procopiou, P. A. *Organometallics* **2007**, 26, 2953–2956. (b) Liu, B.; Roisnel, T.; Carpentier, J.-F.; Sarazin, Y. *Angew. Chem., Int. Ed.* **2012**, 51, 4943–4947. (c) Hu, H.; Cui, C. *Organometallics* **2012**, 31, 1209–1211.
- (13) Tilley, T. D.; Zalkin, A.; Andersen, A. J. *J. Am. Chem. Soc.* **1982**, 104, 3725–3727.
- (14) Basalov, I. V.; Lyubov, D. M.; Fukin, G. K.; Shavyrin, A. S.; Trifonov, A. A. *Angew. Chem., Int. Ed.* **2012**, 51, 3444–3447.
- (15) (a) Heitmann, D.; Jones, C.; Junk, P. C.; Lippert, K. A.; Stasch, A. *Dalton Trans.* **2007**, 187–189. (b) Basalov, I. V.; Lyubov, D. M.; Fukin, G. K.; Cherkasov, A. V.; Trifonov, A. A. *Organometallics* **2013**, 32, 1507–1516.
- (16) Hou, Z.; Zhang, Y.; Tezuka, H.; Xie, P.; Tardif, O.; Koizumi, T.; Yamazaki, H.; Wakatsuki, Y. *J. Am. Chem. Soc.* **2000**, 122, 10533–10543.
- (17) Lee, L.; Berg, D. J.; Bushnell, G. W. *Inorg. Chem.* **1994**, 33, 5302–5308.
- (18) (a) Niemeyer, M. *Eur. J. Inorg. Chem.* **2001**, 1969–1981. (b) Deacon, G. B.; Forsyth, C. M.; Junk, P. C. *Eur. J. Inorg. Chem.* **2005**, 817–821. (c) Evans, W. J.; Champagne, T. M.; Ziller, J. W. *Organometallics* **2007**, 26, 1204–1211.
- (19) (a) Müller-Buschbaum, K.; Quitmann, C. C. *Eur. J. Inorg. Chem.* **2004**, 4330–4337. (b) Evans, W. J.; Rabe, G. W.; Ziller, J. W. *Organometallics* **1994**, 13, 1641–1645.
- (20) Johnson, K. R. D.; Hayes, P. G. *Organometallics* **2011**, 30, 58–67.
- (21) (a) Mansaray, H. B.; Kelly, M.; Vidovic, D.; Aldridge, S. *Chem.—Eur. J.* **2011**, 17, 5381–5386. (b) Moorhouse, R. S.; Moxey, G. J.; Ortu, F.; Reade, T. J.; Lewis, W.; Blake, A. J.; Kays, D. L. *Inorg. Chem.* **2013**, 52, 2678–2683. (c) Blake, A. J.; Lewis, W.; McMaster, J.; Moorhouse, R. S.; Moxey, G. J.; Kays, D. L. *Dalton Trans.* **2011**,



1641–1645. (d) Coombs, N. D.; Stasch, A.; Cowley, A.; Thompson, A. L.; Aldridge, S. *Dalton Trans.* **2008**, 332–337.

(22) Evans, W. J.; Walensky, J. R.; Champagne, T. M.; Ziller, J. W.; DiPasquale, A. G.; Rheingold, A. L. *J. Organomet. Chem.* **2009**, 694, 1238–1243.

(23) Evans, W. J.; Johnston, M. A.; Clark, R. D.; Anwender, R.; Ziller, J. W. *Polyhedron* **2001**, 20, 2483–2490.

(24) Trifonov, A. A.; Kirillov, E. N.; Dechert, S.; Schumann, H.; Bochkarev, M. N. *Eur. J. Inorg. Chem.* **2001**, 2509–2514.

(25) Evans, W. J.; Gummersheimer, T. S.; Boyle, T. J.; Ziller, J. W. *Organometallics* **1994**, 13, 1281–1284.

(26) Hitchcock, P. B.; Khvostov, A. V.; Lappert, M. F.; Protchenko, A. V. *Dalton Trans.* **2009**, 2383–2391.

(27) (a) Tilley, D. T.; Andersen, R. A.; Zalkin, A. *J. Am. Chem. Soc.* **1982**, 104, 3725–3121. (b) Hasinoff, L.; Takats, J.; Zhang, X. W. *J. Am. Chem. Soc.* **1994**, 116, 8833–8834. (c) Deacon, G. B.; Forsyth, C. M. *Chem. Commun.* **2002**, 2522–2523.

(28) Liu, B.; Roisnel, T.; Carpentier, J.-F.; Sarazin, Y. *Chem.—Eur. J.* **2013**, 19.

(29) NMR spectra turned out impossible to integrate when the styrene concentration was higher than 2.61 M.

(30) At very high styrene concentration (4.61 M), the NMR spectra featured very broad resonances, making the integration difficult and inaccurate.

(31) Lyle, S. J.; Rahman, M. M. *Talanta* **1953**, 10, 1177–1182.

(32) Sheldrick, G. M. *SHELXTL v.6.12, Structure Determination Software Suite*; Bruker: Madison, WI, 2000.

(33) Sheldrick, G. M. *SADABS v.2.01, Bruker/Siemens Area Detector Absorption Correction Program*; Bruker: Madison, WI, 1998.